Quantitative three-dimensional evaluation of ablation margins for the prediction of local tumor progression

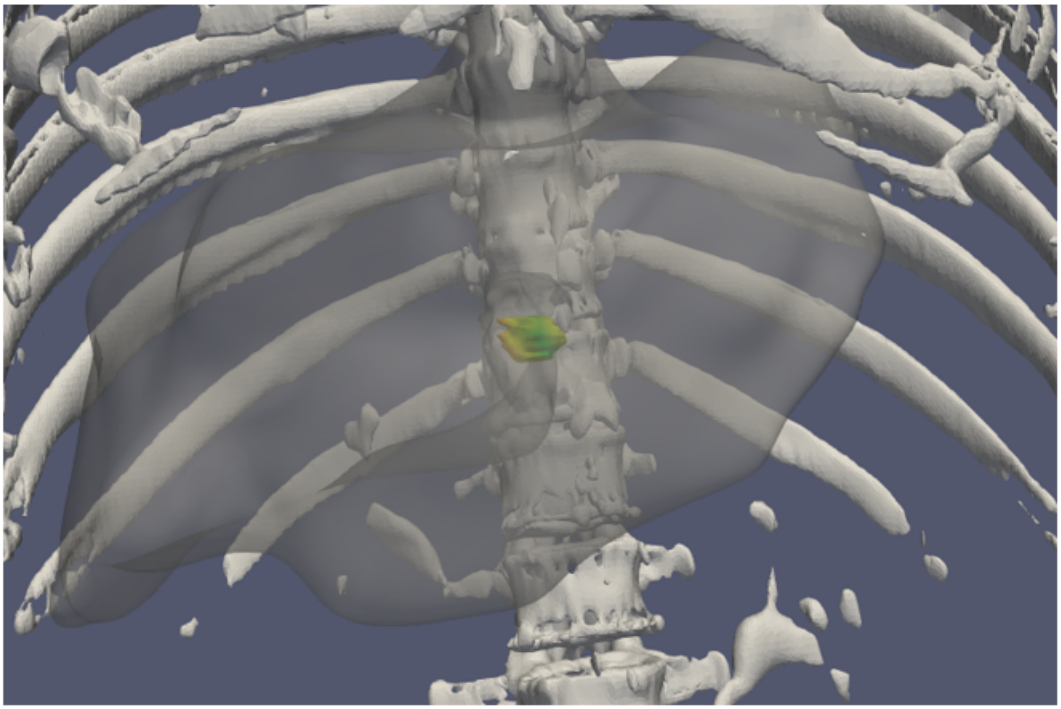

Fleur Boel
Master thesis | Technical Medicine
Imaging & Intervention
September 2019 - September 2020

Leiden University Medical Center

TU Delft Delft University of Technology

Quantitative three-dimensional evaluation of ablation margins for the prediction of local tumor progression

Abstract

Introduction The objective of this research is to assess whether there is a correlation between quantitatively assessed ablation margins and the occurrence of local tumor progression (LTP) using dedicated image processing software.
Methods 28 patients with 45 de novo HCCs treated with percutaneous thermal ablation, e.g. radiofrequency ablation (RFA) and microwave ablation (MWA) between January 2014 and March 2019 were retrospectively included. Semi-automated segmentation of the liver and the ablation zone, manual segmentation of the tumor, and semi-automated registration of pre- and postprocedural contrast enhanced computed tomography (CECT) and magnetic resonance imaging (MRI) images was performed using in-house developed software deLIVERed. The image processing results were used for quantitative analysis of the minimal ablation margin (MAM) and the ablation margin surface area. The outcome of the quantitative analysis was compared to LTP occurence.
Results Image processing of the scans of 39 of the 45 tumors was feasible. 5/39 tumors developed LTP. Based on quantitative analysis, thermal ablation was insufficient in 29/39 tumors. Of these 29 tumors, 4 developed LTP. The median MAM for the LTP group and no LTP group was -4.6 and -1.7 mm, respectively. There was no clear correlation between the MAM and LTP occurrence. The median tumor surface area exposed to insufficient margins was 28.9% and 7.7.% with and without development of LTP, respectively.
Conclusion Quantitative analysis of postablation images can provide insight in ablation margins and the development of LTP. The ablation margin surface area provides additional information to the MAM. However, additional research is needed in order to further investigate the implications of ablation margin surface area.

Introduction

Ablation is a first line treatment in patients with very early and early stage hepatocellular carcinomas (HCCs) [1–3]. In order for ablation to be curative, the tumor needs to be accurately and entirely ablated. Since it is impossible to assess histopathological margins as is done in surgical resection, treatment efficacy of ablation is assessed based on the absence of viable tumor on follow-up imaging. Immediate assessment of treatment success on post-ablation images makes additional ablation within the same procedure feasible.

Most commonly, technical success is evaluated by visual estimation of ablation margins using side-to-side comparison of pre- and postablation images. However, it is difficult to assess ablation margins using side-by-side comparison, especially in 3D [4]. Definitions of technical success used in practice are absence of contrast enhancement and washout in and around the ablation area 0n postablation imaging [5–12], and complete coverage of the tumor by the ablation zone with adequate safety margin [11, 13–20].

The minimal ablation margin (MAM), or safety margin, is often used as a quantitative measure of treatment success. In general, a MAM >5mm is recommended [5–7, 9–11, 13–15, 17, 18, 21–34]. In previous research a MAM <5 mm was associated with a higher rate of local tumor progression (LTP). [24, 26, 30, 35, 36].

Image processing of pre- and postablation images with functions as image overlay and 3D quantification tools may assist in identifying insufficient ablation margins, and help determine technical success. For these analyses, software is used that facilitates the segmentation of the liver volume, tumor and ablation zone; registration of the pre- and postprocedural contrast enhanced computed tomography (CECT) or magnetic resonance imaging (MRI) images; and calculation and depiction of the ablation margins.

Ideally, a standardized ablation margin assessment method with a clear cut-off value that strongly correlates with progression free survival would be available for optimizing thermal ablation practice.

The objective of this research is to assess the diagnostic accuracy of quantitatively assessed minimal ablation margins, and the ablation margin surface area to predict LTP using dedicated image processing software.

Methods

Patients

All patients consecutively treated with percutaneous thermal ablation, e.g. radiofrequency ablation (RFA) and microwave ablation (MWA), for de novo HCC between January 2014 and March 2019 in our institution were identified retrospectively. In total, 130 patients were treated in this period. Exclusion criteria were follow-up less than one year without the development of LTP, liver transplantation within one year of ablation without development of LTP, more than 6 weeks between pre-ablation imaging and treatment, adjuvant treatment with TARE or TACE, or a missing final CECT after ablation, see Table 1. Only radiologically identified LTP was used. 28 patients with 45 tumors were included in this research. Baseline characteristics can be found in Table 2.

Table 1: Exclusion criteria.

Exclusion criteria	*n*
Follow-up <1 year without LTP	24
Liver transplant <1 year without LTP	27
>6 weeks between preprocedural imaging and treatment	30
Adjuvant TARE or TACE	16
Missing final CECT after ablation	5

LTP: Local tumor progression. TARE: transarterial radioembolization. TACE: transarterial chemoembolization. CECT: contrast enhanced computed tomography.

DeLIVERed image processing

Image segmentation and registration were performed using in-house developed software deLIVERed (de Leiden Interactive Visualization En Registration editor, version 1.0), an Elastix based algorithm implemented in MeVisLab. Image processing consisted of three main steps, namely manual segmentation of the tumor, semi-automatic segmentation of the liver, rigid registration of the pre- and postablation images, and semi-automatic segmentation of the ablation zone, see Figure 1. In case of multifocal tumor treatment, image processing was performed for each tumor separately. This allowed for local optimization of the registration around the tumor.

Table 2: Patient characteristics

	n
Treated tumors per patient	
1	17
2	7
3	2
4	2
Age	
Mean (SD)	64.7 (8.7)
Sex	
Male	22
Female	6
Cirrhosis	
Yes	24
No	0
Etiology	
Alcohol abuse	9
Cryptogenic	1
Hepatitis B	8
Hepatitis C	9
Hepatitis D	1
NASH	3
Child Pugh score	
A	19
B	9
BCLC	
Very early	7
Early	17
Intermediate	4
Tumor size (mm)	
Mean (SD)	18.8 (7.7)

NASH: nonalcoholic steatohepatitis. BCLC: Barcelona Clinic for Liver Cancer.

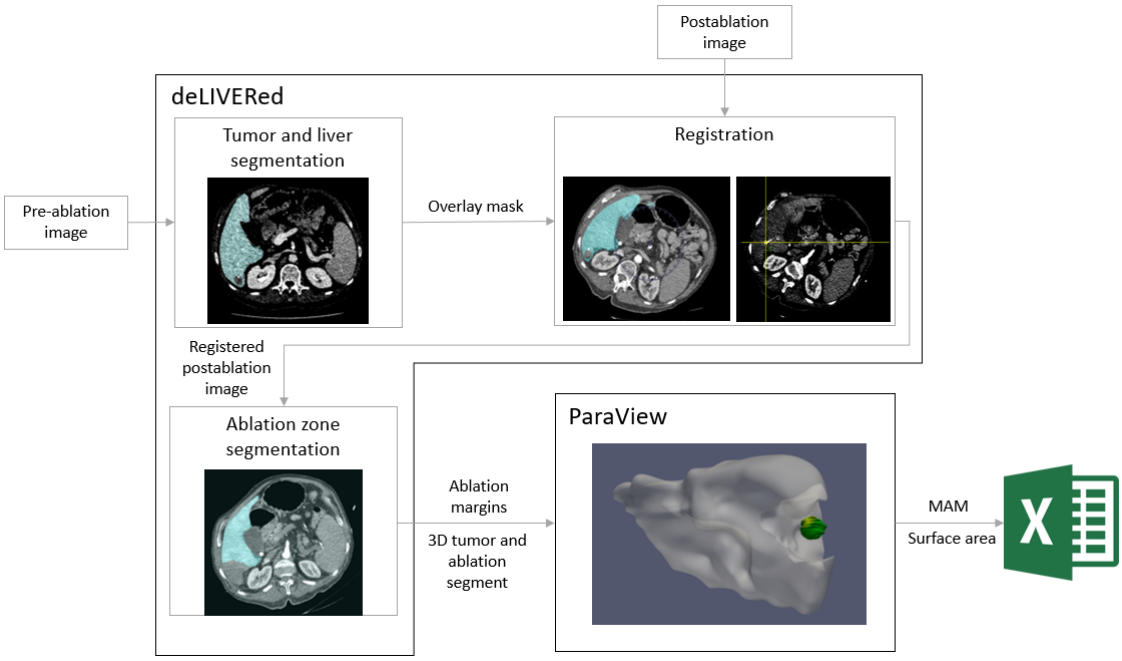

Figure 1: Dataflow used in the quantitative assessment of the minimal ablation margin (MAM) and the ablation margin surface area.

Segmentation of the liver was performed through manual delineation of the liver contour in 5-10 axial 1 mm slices supported by a smart contour algorithm (B-spline). Subsequently, the contours were interpolated to a 3D volume. This 3D volume formed the liver overlay mask, which was used as the volume of interest (VOI) in the registration steps. The tumor segmentation was performed through manual delineation in all axial slices, and then interpolated to a 3D volume. Preferably, the portal venous phase was used for delineation of the tumor. If the observer was not able to delineate the tumor in the portal venous phase, the arterial phase was used. The matching phase was selected from the postablation images to perform the remaining processing steps.

The registration was initiated through initial alignment of the liver mask on the postprocedural CECT image using a manually selected landmark. Manual adjustment of the mask overlay was possible through translation and rotation on the postablation image in all planes. Next, voxel-intensity based rigid registration was performed using adaptive gradient descent Euler transform with a mutual information metric. The registration results were scored by the observer on a 5-point scale, see Table 3.

Table 3: Registration score.

Score	Definition
1	Complete mismatch between the pre- and postprocedural images.
2	Sub-optimal registration with areas of large mismatch around the region of interest.
3	Sufficient registration throughout the liver, although some areas of mismatch around the region of interest make it impossible to make measurements in millimeters.
4	Good registration with ability to make measurements in millimeters, mismatch between pre- and postprocedural images may exist outside the region of interest.
5	Perfect registration with no areas of mismatch around the whole liver.

Manual landmarks could be added to improve the registration results. Landmarks were chosen close to the tumor for local optimization of the registration results. Registration was then repeated with the registration error consisting of the landmark error for 40% and the metric for 60%. The landmark error was calculated using Euclidean distance between the landmarks in the pre- and postablation scan.

After successful registration, the ablation zone was segmented through manual delineation and interpolation. The ablation segment was created by subtraction of the ablation zone from the liver mask. Next, a surface mesh was created for both the segmented tumor and the ablation segment. The ablation margins were calculated for each tumor surface point, and a distance (color)map and a lookup table (LUT) were created. Moreover, the surface area of each tumor surface point was calculated. The colormap and LUT were analyzed using ParaView 5.8.0, and the MAM could be defined.

Image processing was performed by a technical physician and a technical physician in training under supervision of two experienced radiologists. Tumors with registration scores 1-3 were excluded for further analysis as the registrations were too poor to allow per millimeter analysis of the results. The processing result with the best registration score of the two observers was used for further data analysis. A subanalysis was performed including only cases on which both observers scored the registration $\geq$4.

Ablation margin assessment

Image processing allowed for a quantitative analysis of ablation margins. The MAM was defined as the single point with the smallest margin, or the largest insufficient ablation margin. An ablation margin was found to be insufficient if the tumor extended beyond the ablation zone, and the corresponding MAM was then negative. In a second quantitative analysis, the fraction of surface area was evaluated for each ablation margin. Microsoft Excel 2016 was used for the data analysis and creation of figures.

Interobserver analysis

The interobserver analysis was performed for the MAM. The MAM was analyzed through a Bland–Altman plot, which visualizes the difference between the MAM of the two observers against their mean.

Results

Tumors

6/45 tumors in 4/28 patients were excluded from further analysis due to a registration score $\leq$3 (n = 5), or because the tumor could not be delineated properly (n = 1). Registration was impaired in 4/5 excluded tumors in two patients due to rotated post ablation scans and a subcapsular tumor with big differences in respiration mode between pre- and post ablation imaging. 1/5 excluded tumors had artifacts surrounding the tumor location due to a transjugular intrahepatic portosystemic shunt, hindering the registration due to a lack of landmarks in the tumor proximity.

Table 4: Tumor characteristics

	LTP	**No LTP**
	n	*n*
Total	5	34
Tumor size (mm)		
Mean (SD)	24 (6.7)	17.8 (7.2)
Ablation method		
RFA	3	24
MWA	2	10

Table 5: Quantitative assessment of ablation margin.

	LTP	**No LTP**
	n	*n*
Total	5	34
Insufficient ablation margin		
Yes	4	25
No	1	9
Minimal ablation margin [mm]		
Median (range)	-4.6 (-9.4 – 2.0)	-1.7 (-12.5 – 4.7)

RFA: radiofrequency ablation. MWA: microwave ablation.

Local tumor progression

5/39 (12.8%) of tumors developed LTP. Additionally, 5/26 (19.2%) of patients developed distant intrahepatic recurrence. Tumor characteristics were evaluated for tumors with and without development of LTP, see Table 4. No differences were found between the two groups regarding tumor size and thermal ablation method.

Thermal ablation necrosis encompassed the entire tumor in 10/39 (25.6%) of tumors based on the quantitative analysis. Only 1/10 (10%) of tumors developed LTP. The remaining 29/39 (74.4%) tumors all had insufficient margins. Out of these 29 tumors, 4 (13.8%) developed LTP. The median MAM was -4.6 mm and -1.8 mm in the LTP and the no LTP group, respectively, see Figure 2.

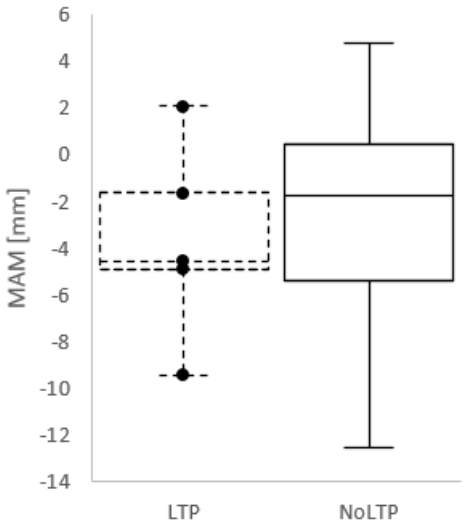

Figure 2: Boxplot of the quantitative minimal ablation margin size for tumors with and without local tumor progression (LTP). The boxplot for the LTP group was added to provide some insight in the data, however the LTP group consists of only five datapoints, and therefore a true boxplot could not be made.

A subset analysis of the MAM was performed using only tumors with a registration score of ≥4 from both observers. 11/39 (28.2%) additional tumors in 11/24 (45.8%) patients were excluded from this subset. 4/28 (14.3%) of the included tumors in the subset analysis developed LTP. The median MAM was -3.1 mm and -1.2 mm in the LTP and the no LTP group, respectively, see Figure 3.

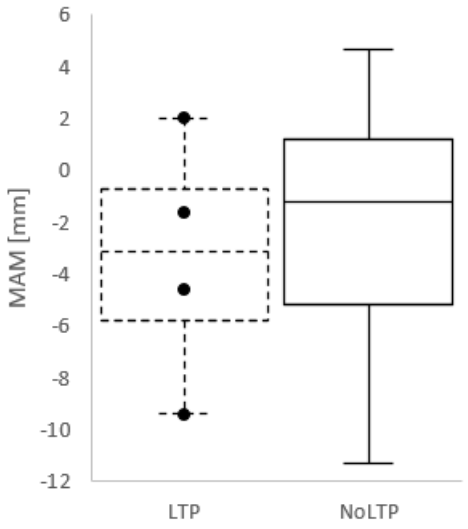

Figure 3: Boxplot of the quantitative minimal ablation margin size for the subset of tumors with and without local tumor progression (LTP). The subset consists of tumors which received a registration score of ≥4 from both observers. The boxplot for the LTP group was added to provide some insight in the data, however the LTP group consists of only four datapoints, and therefore a true boxplot could not be made.

Cumulative ablation margin surface area

In Figure 4, two cases with insufficient margins are depicted, one case with LTP and one case without. The ablation margin surface area can provide additional information about the determined ablation margins. The median cumulative ablation margin surface area is depicted in Figure 6. The median cumulative ablation margin surface area for margins ≤0 mm is 28.9% and 7.7% for tumors with and without LTP, respectively. If a cut-off value of 5% cumulative ablation margin surface area for margins ≤0 mm is used, a sensitivity of 0.8 and specificity of 0.47 for the prediction of LTP were found. Based on these data, to avoid 80% of all LTP cases, approximately half of the tumors not prone to development of LTP would be treated with additional ablation. Consequently, approximately half of the tumors would receive unnecessary treatment.

The median cumulative ablation margin surface area for margins ≤5 mm is 85.2% and 64.4% for tumors with and without LTP, respectively. If a cut-off value of 40% cumulative ablation margin surface area for margins ≤5 mm is used, a sensitivity of 1.0 and specificity of 0.24 is found.

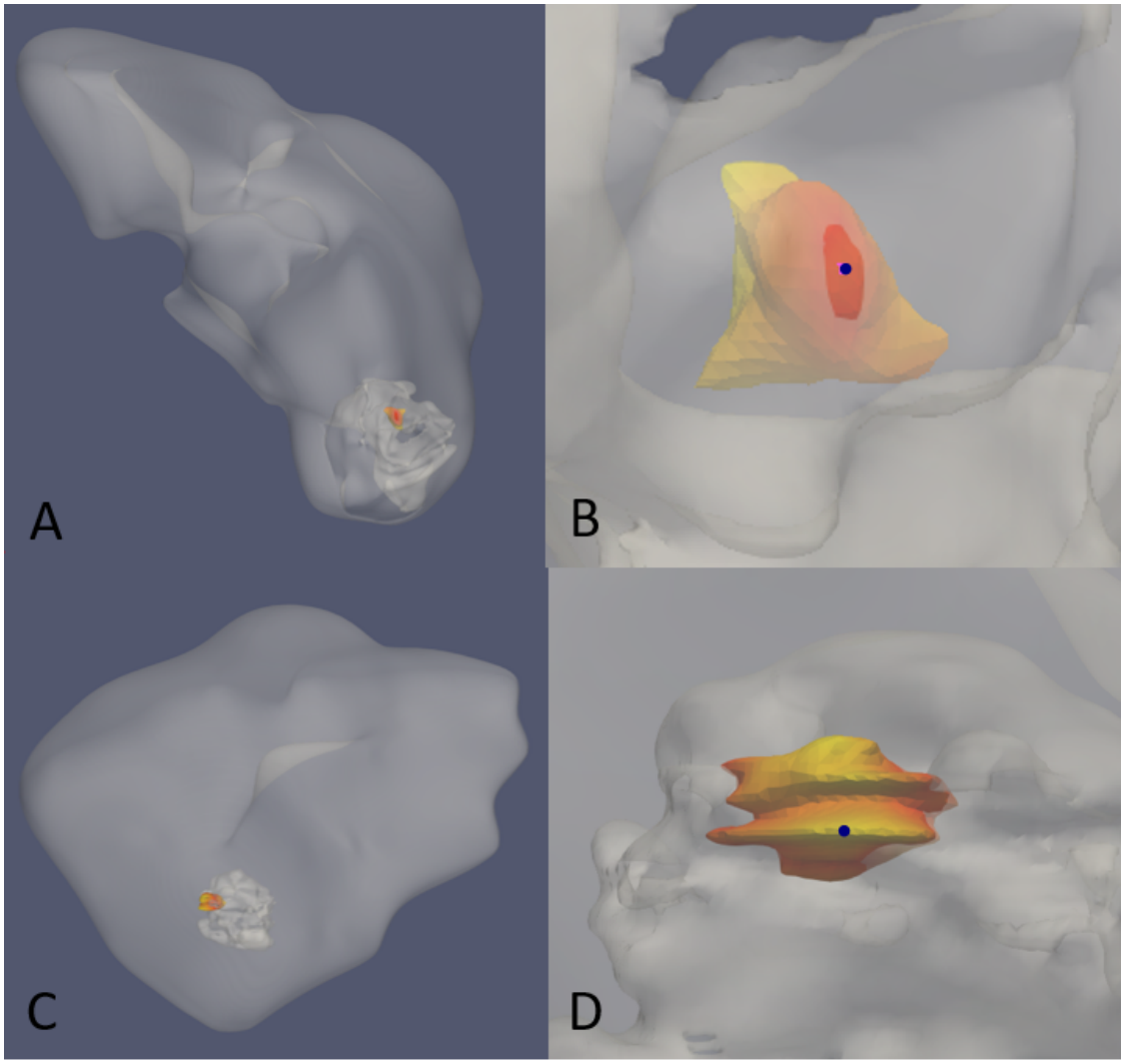

Figure 4: Two cases with insufficient ablation margins as determined through quantitative analysis. A: Example tumor with insufficient margins and no development of local tumor progression (LTP). B: Close-up of the no LTP case. The minimal ablation margin (MAM) in blue, surrounded by the surface area with insufficient margin, which is demarcated by the ablation zone surface (gray). C: Example tumor with insufficient margins and development of LTP. D: Close-up of the LTP case. The MAM in blue, surrounded by the surface area with insufficient margin, which encompasses almost the entire visible face of the tumor.

This leads to overtreatment of approximately 75% of the tumors in order to avoid 100% of LTP cases, based on these data. If a cut-off value of 34% cumulative ablation margin surface area for margins $\leq$5 mm is used, a sensitivity of 0.8 and specificity of 0.29 is found. This would lead to overtreatment of approximately 70% of the tumors in order to avoid 100% of LTP cases, based on these data.

Interobserver analysis

19 tumors where included in the interobserver analysis of the MAM. The mean error was 1.5 mm (SD 3.5 mm). The interobserver Bland Altman plot is depicted in Figure 5.

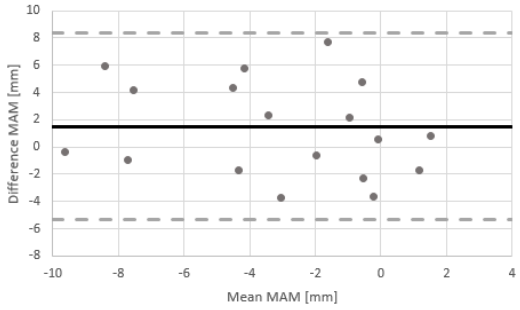

Figure 5: Interobserver Bland Altman plot for the minimal ablation margin (MAM), with the mean error (black) and the 95% CI (dashed gray).

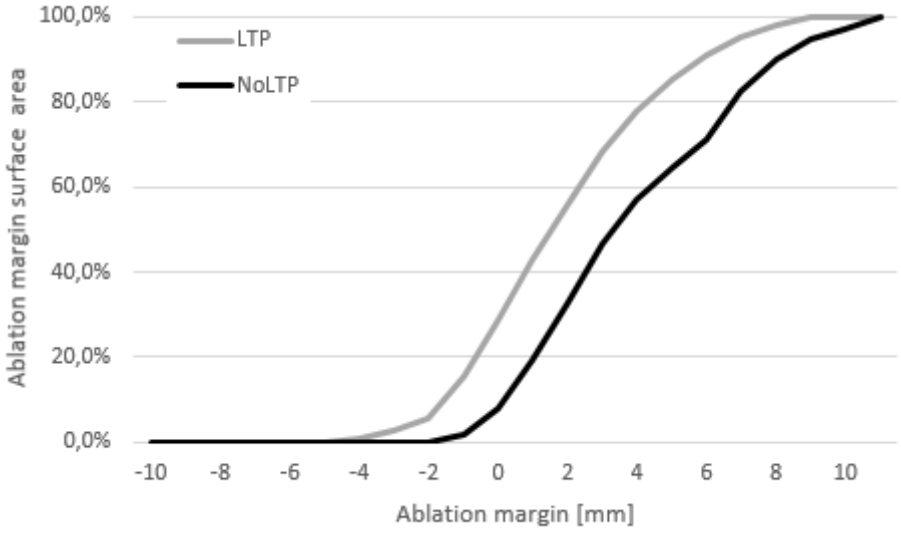

Figure 6: The median cumulative ablation margin surface area for tumors with and without local tumor progression (LTP).

Discussion

In this retrospective study, quantitative assessment of the MAM and cumulative ablation margin surface area was performed using in house developed software deLIVERed. There was no clear correlation between the MAM and LTP occurrence. The median MAM for the LTP group and no LTP group was -4.6 and -1.7 mm, respectively. In the subset analysis for tumors with a registration score $\geq$4 from both observers, the median MAM for the LTP group and no LTP group was -3.1 and -1.2 mm, respectively. This method of quantitative evaluation does not take intraprocedural tumor shrinkage into account. RFA and MWA necrosis volumes are influenced by tissue shrinkage, which is inhomogeneous and unpredictable [37–43]. Hence, a tumor with a small negative minimal ablation margin in the quantitative analysis may still be treated sufficiently. Tumor surface area exposed to insufficient margins may therefore be a better measure for treatment success. The median tumor surface area exposed to insufficient margins was 28.9% and 7.7.% with and without development of LTP, respectively. Solbiati et al. [18] assessed the tumor surface area exposed to an ablation margin $\leq$5 mm in 50 patients after MWA. The software uses automatic segmentation of the liver, semi-automated segmentation of the tumor and the ablation zone, and non-rigid registration of the pre- and post-procedural images. 21/90 (23%) tumors developed local tumor progression. 13/17 (77%) tumors with an insufficient ablation margin developed LTP. No further analysis of the size of the tumor surface area with insufficient margins was performed. All other tumors with LTP had complete tumor ablation with a margin of at least 5 mm on 0-99 % of the tumor surface area. If the tumors with insufficient margins where treated additionally based on these findings, 62% of the LTP cases could be avoided. However, 6% of tumors would be overtreated. Hocquelet et al. [24] calculated the 3D tumor surface area exposed to a margin $\leq$5 mm in eighth patients with LTP and eighth matched patients based on tumor size and α-fetoprotein level. Patients with a tumor surface area $>$425 mm^2 had a 2-year LTP rate of 77.5%, and patients with a tumor surface area $\leq$ 425 mm^2 had a 2-year LTP rate of 25%. When using 425 mm^2 of the tumor surface area exposed to a margin $\leq$5 mm, 77.5% of the LTP cases could be avoided. By utilizing quantitative analysis of tumor surface area exposed to insufficient margins intraprocedural, areas at risk to local tumor progression can be identified and additional ablation can be performed. The cutt-off value for tumor surface area is dependent on the software used for quantitative analysis. A high sensitivity and specificity are needed in order to identify the cases at risk to LTP, while preventing overtreatment.

In this research, the image processing was performed by two observers. The interobserver analysis of the MAM showed a mean error of 1.5 mm (SD 3.5 mm). Factors influencing the mean error are the delineation of the tumor, the delineation of the liver, the registration and the delineation of the ablation zone. In previous research using this software, the interobserver variability was also evaluated, where only the registration and segmentation of the ablation zones were performed by two different observers [44]. There, a

mean error of -1.06 mm (SD: 2.19) was found. The difference in found interobserver variability in this study might be due to the addition of the tumor delineation. In order to get more insight in the different aspects of the image processing on the mean error, additional interobserver analyses need to be performed. The influence of the tumor delineation can be investigated through delineation by a different observer, followed by registration and segmentation of the ablation zone by one experienced observer. Due to the current workflow of the software, where first the registration is performed, and where the preprocedural image is used as the fixed image, it is not possible to separate the registration and segmentation of the ablation zone.

In this research, manual and semi-automated segmentation and semi-automated rigid registration were used. Segmentation was performed manually for the tumor, and semi-automatically for the liver and ablation zone. Interobserver variability can be reduced through implementation of automated registration methods. Registration was performed for each tumor individually in the case of multi-focal tumor treatment, in order to create locally optimized registration results. The rigid registration was impossible to perform in 5/45 (11%) tumors. In 4/5 tumors this was due to rotation of the postprocedural scan and a subcapsular tumor location. The difference in patient orientation and respiration mode causes large deformations to the tumor. If there is a lack of usable landmarks near the tumor, as was the case for these tumors, it is impossible to make an locally optimized registration. To reduce liver deformation, pre-and postablation are best performed immediately before and after ablation with the patient under general anesthesia using high-jet ventilation or full expiration during scanning.

In literature, a mixture of manual and automated methods are described for rigid and non-rigid registration. Rigid registration provides a fast method, with accurate locally optimized registration if intrahepatic landmarks are available near the tumor which are visible on both pre- and postablation images. Non-rigid registration is more suitable for full liver registration, since the liver is deformed due to breathing and patient positioning. However, non-rigid registration takes long to compute and it adds an average image deformation of 5.1 mm and 7.2 mm for patients with and without different orientation and respiratory phase, respectively [45]. The choice of registration method is therefore in part dependent on the workflow and desired end result of registration.

Limitations of this study are its retrospective design and the small number of tumors, especially the number of tumors developing LTP. The LTP rate of 12.8% found in this study is lower than comparable studies in literature [18, 46]. This is in part caused by the inclusion of only radiologically identified LTP. 27/102 (26.5%) patients excluded from this study undergo liver transplantation. Inclusion of pathologically proven LTP after liver transplant in further research is therefore needed to create a bigger and more representative cohort. The low LTP occurrence resulted in a small LTP group, which meant no statistical analysis could be performed. Moreover, the outcome of the quantitative analysis is influenced by multiple factors. These factors include the skill of the observer, the availability of landmarks near the tumor, the tumor location, the patient positioning and breathing phase in each of the images, the registration quality and the segmentation quality.

Conclusion

Quantitative analysis of postablation images can provide insight in ablation margins and the development of LTP. The ablation margin surface area provides additional information to the MAM. However, additional research is needed in order to further investigate the implications of ablation margin surface area. In order to implement quantitative analysis of ablation margins in practice, a clear understanding of the software, a suitable workflow, and a cut-off value of the minimal ablation margin and the ablation margin surface area with sufficient sensitivity and specificity are needed. The deLIVERed software therefore needs to be tested further in a large prospective study.

References

[1] European Association for the Study of the Liver. EASL Clinical Practice Guidelines: Management of hepatocellular carcinoma. J Hepatol. 2018;69(1):182–236.

[2] Roberts S, Gazzola A, Lubel J, Gow P, Bell S, Nicoll A, et al. Treatment choice for early-stage hepatocellular carcinoma in real-world practice: impact of treatment stage migration to transarterial chemoembolization and treatment response on survival. Scand J Gastroenterol. 2018;53(10–11):1368–1375.

[3] Forner A, Reig M, Bruix J. Hepatocellular carcinoma. Lancet. 2018;391(10127):1301–1314.

[4] Schraml C, Clasen S, Schwenzer N, Koenigsrainer I, Herberts T, Claussen C, et al. Diagnostic performance of contrast-enhanced computed tomography in the immediate assessment of radiofrequency ablation success in colorectal liver metastases. Abdom Imaging. 2008;33(6):643–651.

[5] Cha D, Kang T, Song K, et al. Radiofrequency ablation for subcardiac hepatocellular carcinoma: therapeutic outcomes and risk factors for technical failure. Eur Radiol. 2019;29(5):2706–2715.

[6] El-Gendi A, El-Shafei M, Abdel-Aziz F, Bedewy E. Intraoperative ablation for small HCC not amenable for percutaneous radiofrequency ablation in Child A cirrhotic patients. Gastrointest Surg. 2013;17(4):712–718.

[7] Koh Y, Choi J, Kim H, Kim M. Computed tomographic-guided radiofrequency ablation of recurrent or residual hepatocellular carcinomas around retained iodized oil after transarterial chemoembolization. Korean J Radiol. 2013;14(5):733–742.

[8] Laimer G, Schullian P, Jaschke N, et al. Minimal ablative margin (MAM) assessment with image fusion: an independent predictor for local tumor progression in hepatocellular carcinoma after stereotactic radiofrequency ablation [published online ahead of print, 2020 Jan 30]. Eur Radiol. 2020;10.1007:s00330–019–06609–7.

[9] Lee M, Kim Y, Park S, et al. Biplane fluoroscopy-guided radiofrequency ablation combined with chemoembolisation for hepatocellular carcinoma: initial experience. Br J Radiol. 2011;84(1004):691–697.

[10] Li X, Fan W, Zhang L, et al. CT-guided percutaneous microwave ablation of liver metastases from nasopharyngeal carcinoma. J Vasc Interv Radiol. 2013;24(5):680–684.

[11] Sibinga Mulder B, Hendriks P, Baetens T, et al. Quantitative margin assessment of radiofrequency ablation of a solitary colorectal hepatic metastasis using MIRADA RTx on CT scans: a feasibility study. BMC Med Imaging. 2019;19(1):71.

[12] Zhang Q, Li X, Pan J, Wang Z. Transpulmonary computed tomography-guided radiofrequency ablation of liver neoplasms abutting the diaphragm with multiple bipolar electrodes. Indian J Cancer. 2015;52 Suppl 2:e64–e68.

[13] Choi J, Lee J, Lee D, et al. Switching Monopolar Radiofrequency Ablation Using a Separable Cluster Electrode in Patients with Hepatocellular Carcinoma: A Prospective Study. PLoS One. 2016;11(8):e0161980.

[14] Kamei S, Matsuda J, Hagihara M, et al. Oblique approach for CT-guided liver radiofrequency ablation using multiplanar reformation images in hepatocellular carcinoma. Jpn J Radiol. 2012;30(6):533–539.

[15] Kim Y, Lee W, Rhim H, Lim H, Choi D, Lee J. The minimal ablative margin of radiofrequency ablation of hepatocellular carcinoma ($>$ 2 and $<$ 5 cm) needed to prevent local tumor progression: 3D quantitative assessment using CT image fusion. AJR Am J Roentgenol. 2010;195(3):758–765.

[16] Makino Y, Imai Y, Igura T, et al. Utility of computed tomography fusion imaging for the evaluation of the ablative margin of radiofrequency ablation for hepatocellular carcinoma and the correlation to local tumor progression. Hepatol Res. 2013;43(9):950–958.

[17] Park S, Kim I, Lee S, et al. Angled CoolTip Electrode for Radiofrequency Ablation of Small Superficial Subcapsular Tumors in the Liver: A Feasibility Study. Korean J Radiol. 2016;17(5):742–749.

[18] Solbiati M, Muglia R, Goldberg S, et al. A novel software platform for volumetric assessment of ablation completeness. Int J Hyperthermia. 2019;36(1):337–343.

[19] Vo Chieu V, Werncke T, Hensen B, Wacker F, Ringe K. CT-Guided Microwave Ablation of Liver Tumors in Anatomically Challenging Locations. Cardiovasc Intervent Radiol. 2018;1520–1529(41):10.

[20] Wang X, Sofocleous C, Erinjeri J, et al. Margin size is an independent predictor of local tumor progression after ablation of colon cancer liver metastases. Cardiovasc Intervent Radiol. 2013;36(1):166–175.

[21] Abdel-Rehim M, Ronot M, Sibert A, Vilgrain V. Assessment of liver ablation using cone beam computed tomography. World J Gastroenterol. 2015;21(2):517–524.

[22] Cazzato R, Garnon J, Ramamurthy N, et al. 18F-FDOPA PET/CT-Guided Radiofrequency Ablation of Liver Metastases from Neuroendocrine Tumours: Technical

Note on a Preliminary Experience. Cardiovasc Intervent Radiol. 2016;39(9):1315–1321.

[23] Fukuda K, Mori K, Hasegawa N, et al. Safety margin of radiofrequency ablation for hepatocellular carcinoma: a prospective study using magnetic resonance imaging with superparamagnetic iron oxide. Jpn J Radiol. 2019;37(3):555–563.

[24] Hocquelet A, Trillaud H, Frulio N, et al. Three-Dimensional Measurement of Hepatocellular Carcinoma Ablation Zones and Margins for Predicting Local Tumor Progression. J Vasc Interv Radiol. 2016;27(7):1038–1045.

[25] Iwazawa J, Ohue S, Hashimoto N, Mitani T. Ablation margin assessment of liver tumors with intravenous contrast-enhanced C-arm computed tomography. World J Radiol. 2012;4(3):109–114.

[26] Jiang C, Liu B, Chen S, Peng Z, Xie X, Kuang M. Safety margin after radiofrequency ablation of hepatocellular carcinoma: precise assessment with a three-dimensional reconstruction technique using CT imaging. Int J Hyperthermia. 2018;34(8):1135–1141.

[27] Kang T, Rhim H, Lee J, et al. Magnetic resonance imaging with gadoxetic acid for local tumour progression after radiofrequency ablation in patients with hepatocellular carcinoma. Eur Radiol. 2016;26(10):3437–3446.

[28] Liao M, Zhong X, Zhang J, et al. Radiofrequency ablation using a 10-mm target margin for small hepatocellular carcinoma in patients with liver cirrhosis: A prospective randomized trial. J Surg Oncol. 2017;115(8):971–979.

[29] Liu Z, Chang Z, Lu Z, Guo Q. Early PET/CT after radiofrequency ablation in colorectal cancer liver metastases: is it useful? Chin Med J (Engl). 2010;123(13):1690–1694.

[30] Motoyama T, Ogasawara S, Chiba T, et al. Coronal reformatted CT images contribute to the precise evaluation of the radiofrequency ablative margin for hepatocellular carcinoma. Abdom Imaging. 2014;39(2):262–268.

[31] Park Y, Choi D, Rhim H, et al. Central lower attenuating lesion in the ablation zone on immediate follow-up CT after percutaneous radiofrequency ablation for hepatocellular carcinoma: incidence and clinical significance. Eur J Radiol. 2010;75(3):391–396.

[32] Sakakibara M, Ohkawa K, Katayama K, et al. Three-dimensional registration of images obtained before and after radiofrequency ablation of hepatocellular carcinoma to assess treatment adequacy. AJR Am J Roentgenol. 2014;202(5):W487–W495.

[33] Shin S, Lee J, Kim K, et al. Postablation assessment using follow-up registration of CT images before and after radiofrequency ablation (RFA): prospective evaluation of midterm therapeutic results of RFA for hepatocellular carcinoma. AJR Am J Roentgenol. 2014;203(1):70–77.

[34] Takeyama N, Mizobuchi N, Sakaki M, et al. Evaluation of hepatocellular carcinoma ablative margins using fused pre- and post-ablation hepatobiliary phase images. Abdom Radiol (NY). 2019;44(3):923–935.

[35] Kei S, Rhim H, Choi D, Lee W, Lim H, Kim Y. Local tumor progression after radiofrequency ablation of liver tumors: analysis of morphologic pattern and site of recurrence. AJR Am J Roentgenol. 2008;190(6):1544–1551.

[36] Nakazawa T, Kokubu S, Shibuya A, et al. Radiofrequency ablation of hepatocellular carcinoma: correlation between local tumor progression after ablation and ablative margin. AJR Am J Roentgenol. 2007;188(2):480–488.

[37] Amabile C, Farina L, Lopresto V, et al. Tissue shrinkage in microwave ablation of liver: an ex vivo predictive model. Int J Hyperthermia. 2017;33(1):101–109.

[38] Brace C. Tissue contraction caused by radiofrequency and microwave ablation: a laboratory study in liver and lung. J Vasc Interv Radiol. 2010;21(8):1280–1286.

[39] Farina L, Weiss N, Nissenbaum Y, et al. Characterisation of tissue shrinkage during microwave thermal ablation. Int J Hyperthermia. 2014;30(7):419–428.

[40] Lee J, Siripongsakun S, Bahrami S, Raman S, Sayre J, Lu D. Microwave ablation of liver tumors: degree of tissue contraction as compared to RF ablation. Abdom Radiol (NY). 2016;41(4):659–666.

[41] Liu D, Brace C. CT imaging during microwave ablation: analysis of spatial and temporal tissue contraction. Med Phys. 2014;41(11):113303.

[42] Rossmann C, Garrett-Mayer E, Rattay F, Haemmerich D. Dynamics of tissue shrinkage during ablative temperature exposures. Physiol Meas. 2014;35(1):55–67.

[43] Weiss N, Goldberg S, Nissenbaum Y, Sosna J, Azhari H. Planar strain analysis of liver undergoing microwave thermal ablation using x-ray CT. Med Phys. 2015;42(1):372–380.

[44] Willink Y. Performance evaluation of de Leiden Interactive Visualization En Registration editor (deLIVERed): a software development study. Available at: Leiden University Medical Center - department of Radiology;.

[45] Luu H, Moelker A, Klein S, Niessen W, van Walsum T. Quantification of nonrigid liver deformation in radiofrequency ablation interventions using image registration. Phys Med Biol. 2018;63(17):175005.

[46] Hendriks P, Noortman W, Baetens T, et al. Quantitative Volumetric Assessment of Ablative Margins in Hepatocellular Carcinoma: Predicting Local Tumor Progression Using Nonrigid Registration Software. J Oncol. 2019;2019:4049287.